8882 *Biochemistry* **2010,** *49,* 8882–8891
DOI: 10.1021/bi1009979

BIOCHEMISTRY
including biophysical chemistry & molecular biology
Article

Key Dynamics of Conserved Asparagine in a Cryptochrome/Photolyase Family Protein by Fourier Transform Infrared Spectroscopy[†]

Tatsuya Iwata,[‡,§] Yu Zhang,[‡] Kenichi Hitomi,[∥,⊥] Elizabeth D. Getzoff,[∥] and Hideki Kandori*[,‡]

[‡]*Department of Frontier Materials, Nagoya Institute of Technology, Showa-ku, Nagoya 466-8555, Japan,* [§]*Center for Fostering Young and Innovative Researchers, Nagoya Institute of Technology, Showa-ku, Nagoya 466-8555, Japan,* [∥]*Department of Molecular Biology and Skaggs Institute for Chemical Biology, The Scripps Research Institute, La Jolla, California 92037, and* [⊥]*Life Sciences Division, Lawrence Berkeley National Laboratory, Berkeley, California 94720*

Received June 21, 2010; Revised Manuscript Received September 9, 2010

ABSTRACT: Cryptochromes (Crys) and photolyases (Phrs) are flavoproteins that contain an identical cofactor (flavin adenine dinucleotide, FAD) within the same protein architecture but whose physiological functions are entirely different. In this study, we investigated light-induced conformational changes of a cyanobacterium Cry/Phr-like protein (*S*Cry-DASH) with UV−visible and Fourier transform infrared (FTIR) spectroscopy. We developed a system for measuring light-induced difference spectra under the concentrated conditions. In the presence of a reducing agent, *S*Cry-DASH showed photoreduction to the reduced form, and we identified a signal unique for an anionic form in the process. Difference FTIR spectra enabled us to assign characteristic FTIR bands to the respective redox forms of FAD. An asparagine residue, which anchors the FAD embedded within the protein, is conserved not only in the cyanobaterial protein but also in Phrs and other Crys, including the mammalian clock-related Crys. By characterizing an asparagine-to-cysteine (N392C) mutant of *S*Cry-DASH, which mimics an insect specific Cry, we identified structural changes of the carbonyl group of this conserved asparagine upon light irradiation. We also found that the N392C mutant is stabilized in the anionic form. We did not observe a signal from protonated carboxylic acid residues during the reduction process, suggesting that the carboxylic acid moiety would not be directly involved as a proton donor to FAD in the system. These results are in contrast to plant specific Crys represented by *Arabidopsis thaliana* Cry1 that carry Asp at the position. We discuss potential roles for this conserved asparagine position and functional diversity in the Cry/Phr frame.

Members of the cryptochrome/photolyase family of proteins are found throughout all three kingdoms of life, from bacteria to archaea to animals, including humans (*1*, *2*). Cryptochromes (Crys)[1] and photolyases (Phrs) share an identical chromophore (flavin adenine dinucleotide, FAD) within a homologous protein architecture termed a Phr-like domain (*1*) (Figure 1a−d). Despite structural homology, their physiological functions are quite distinct. Phrs repair ultraviolet (UV)-induced photoproducts in DNA using near-UV and blue light with the cofactor. In higher organisms, Phr-like gene products, termed Cry to distinguish them from the DNA repair Phrs, also function in a light-dependent manner but control growth or regulate flowering time in plants and maintain circadian rhythms in animals (*3*). For Crys, redox of FAD has been debated (*4*, *5*); however, contributions of FAD to the signaling still remain enigmatic. Even for the better-characterized Phrs, the means by which FAD redox changes result in downstream protein dynamics are still poorly understood.

The Cry/Phr family is categorized into two major classes. Cryptochrome-DASH (Cry-DASH) is a newly found cluster of proteins belonging to the class I family (*6*). While the gene clusters of animal and plant Crys homologous are literally found in the respective kingdoms, Cry-DASH-type genes are found in all kingdoms, bacteria, plants (*6*), and also some vertebrates (*7*). Although specific physiological functions in individual organisms are still unclear, Cry-DASH proteins are likely photoreceptors, as the proteins contain two light-harvesting cofactors, FAD and 5,10-methenyltetrahydrofolate, and the light-dependent DNA repair activity is negligible in vivo (*6*, *8*), retaining repair activity for single-stranded DNA in vitro (*9*, *10*). On the other hand, Phr is a photoreceptor in a way (*11*). Originally, genes belonging to the cluster were discovered in *Synechocystis* sp. PCC6803 and *Arabidopsis thaliana*; however, the overall structural features of the encoded proteins are in fact more similar to those of *Homo sapiens* and *Drosophila* Crys than those of prototypical plant Crys containing characteristic long C-termini. These Cry-DASH proteins additionally provide relatively good yields in recombinant bacterial expression systems, and several X-ray crystal structures of Cry-DASH derived from *Synechocystis* sp. and *Arabidopsis* have been reported (*12*, *13*) (Figure 1a). Cry-DASH proteins are therefore a good model for studying Crys and Phrs using spectroscopic methods.

[†]This work was supported by grants from Japanese Ministry of Education, Culture, Sports, Science, and Technology to H.K. (20050015 and 20108014) and National Institutes of Health Grant GM37684 (E.D.G.). K.H. was supported by the Skaggs Institute for Chemical Biology.

*To whom correspondence should be addressed: Department of Frontier Materials, Nagoya Institute of Technology, Showa-ku, Nagoya 466-8555, Japan. Phone and fax: 81-52-735-5207. E-mail: kandori@nitech.ac.jp.

[1]Abbreviations: Cry, cryptochrome; Phr, photolyase; FAD, flavin adenine dinucleotide; $FADH^-$, reduced form of FAD; FAD^{ox}, oxidized form of FAD; $FADH^•$, neutral semiquinoid form of FAD; $FAD^{•-}$, anionic form of FAD; FTIR, Fourier transform infrared; BLUF, sensor of blue light using FAD; LOV, light, oxygen, and voltage; FMN, flavin mononucleotide; UV−vis, ultraviolet−visible; PDB, Protein Data Bank.

 Published on Web 09/09/2010

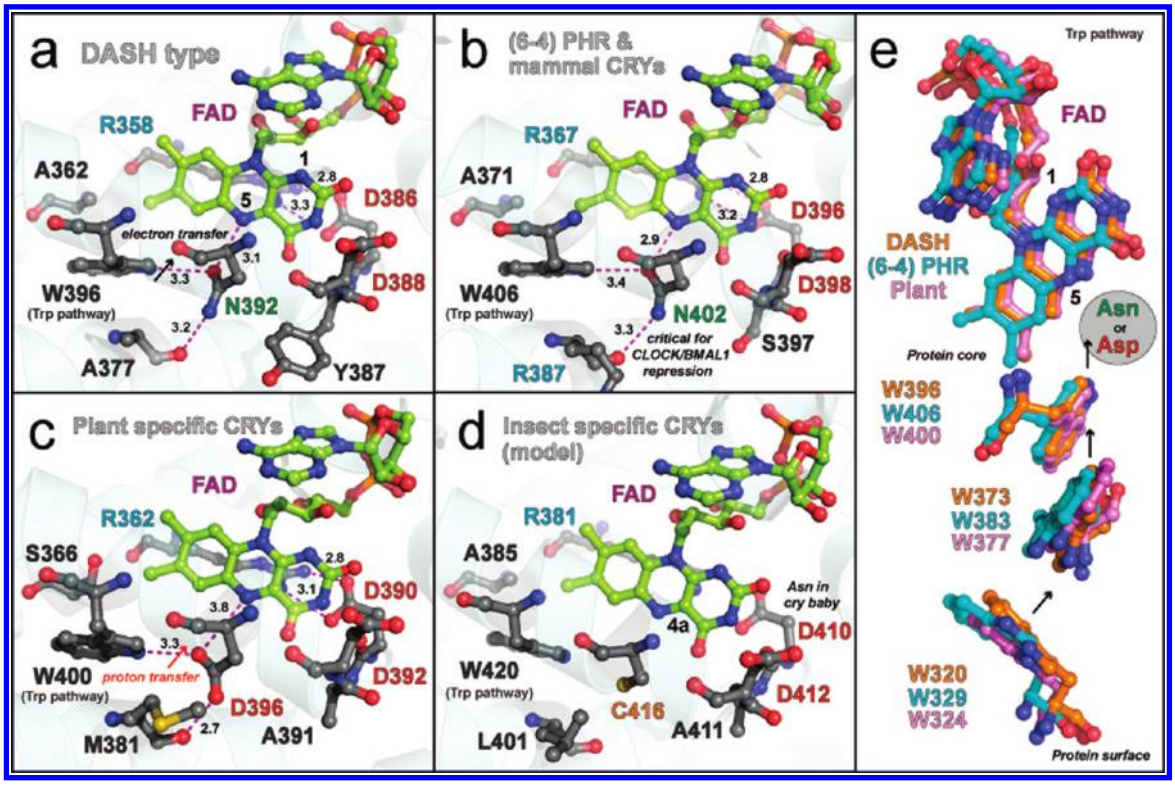

FIGURE 1: Conservation and unique tuning in FAD binding domains of the photolyase and cryptochrome family proteins. Crystal structures of *S*Cry-DASH (a), *Arabidopsis* (6−4) Phr (b), *Arabidopsis* Cry1 (c), and a homology model of *Drosophila* Cry (d) show conservation at the FAD binding sites and indicate the unique tuning. The Cry/Phr proteins have two Asp residues at the FAD binding site (Asp386 and Asp388 in *S*Cry-DASH). One of the Asp residues forms a salt bridge with Arg across the isoalloxazine ring system. The salt bridge is invariant in all Cry/Phr family members. Many Crys and Phrs have a conserved asparagine at the location of Asn392 in *S*Cry-DASH, the region in which the polypeptide chains anchor the cofactor at N5 of isoalloxazine (a and b), whereas plant and insect specific Crys have Asp and Cys, respectively, at the position (c and d). FAD is colored yellow, and critical distances are shown in angstroms with magenta dotted lines. Representatives of each gene cluster of the family, a summary of the conservation in the region, and coordinates used are listed in Table 1. The homology model of *Drosophila* Cry was built with SWISS-MODEL (http://swissmodel.expasy.org) based on *Drosophila* (6−4) Phr (Protein Data Bank entry 3CVV). (e) The Trp triad pathway contributing to the FAD redox is also conserved in the Cry/Phr family. *S*Cry-DASH is colored orange, *Arabidopsis* (6−4) Phr blue, and *Arabidopsis* Cry1 pink. In panel e, molecules were rotated 60° from the views in panels a−c. Structures were drawn with PyMOL (*57*).

The photoreduction and oxidation processes of Cry-DASH have previously been investigated by UV−vis spectroscopy for zebrafish (*14*), *Xenopus laevis* (*15*), and *Synechocystis* sp. (*16*). EPR analyses of mutant Cry-DASH from *X. laevis* have also been successful (*15*, *17*). Phrs appear to use the reduced $FADH^-$ as a redox-active cofactor in the DNA repairs, whereas the oxidized (FAD^{ox}) and neutral semiquinoid ($FADH^\bullet$) forms are inactive (*18*). For at least a few Crys, on the other hand, different FAD chemistry has been reported. For example, in *Arabidopsis* Cry1, the FAD^{ox} form has been proposed as an unphotolyzed state (*4*, *5*). Light-dependent reduction from FAD^{ox} to $FADH^\bullet$ and/or $FADH^-$ is believed to trigger the signaling. Furthermore, the anionic form ($FAD^{\bullet-}$) has been observed in insect Cry (*19*, *20*). Regardless of the cofactor redox chemistry though, all proteins belonging to the Cry/Phr family contain the conserved "Trp triad" and exhibit light-dependent function FAD reduction in the presence of reducing agents (Figure 1e) (*15*).

The amino acid adjacent to the N5 atom of the FAD isoalloxazine ring is considered a key signal transduction residue in flavoproteins. For example, in the LOV (light, oxygen, and voltage) domain of the plant blue light photoreceptor phototropin, whose chromophore is FMN, a cysteine is located near the C4a position of the FMN isoalloxazine ring (*21*−*24*), and a neutral glutamine in the β-sheet anchors the N5 position (*25*). Upon light excitation, the cysteine residue forms a covalent bond with the isoalloxazine ring at the C4a position. Simultaneously, the glutamine residue changes its hydrogen-bonding partner from the C4═O group to the N5−H group, resulting in local structural changes that transmit the light signal downstream of the protein through a β-sheet (*26*) and/or so-called Jα helix (*27*−*29*). Though the Gln residue itself is not necessary for the normal photoreaction, it is important for the structural changes in the signal transduction. Similarly, the BLUF (sensor of blue light using FAD) domain has a Gln nearby the FAD isoalloxazine N5 position, which has been shown to have a critical role in light signal conversion (formation of the red-shifted intermediate) (*30*−*32*).

The amino acid adjacent to FAD isoalloxazine N5 appears to be conserved in Cry/Phr proteins as well, and interestingly, most family members, including mammalian and DASH-type Crys, have an Asn at this position (Figure 1a,b). However, plant Crys (e.g., *Arabidopsis* Cry1) have an Asp, and insect specific Crys have Cys instead (Figure 1c,d and Table 1) (*13*, *19*). A study comparing midpoint redox potentials among FAD redox species for CPD Phrs and *Arabidopsis* Cry1 suggested that this amino acid residue (Asn and Asp, respectively) plays an important role in the control of the FAD redox state (*33*). In addition, a mutant of *Escherichia coli* DNA Phr whose Asn was replaced with other amino acids displays defects in DNA repair activity (*34*). Our recent studies further showed that substitution of the Asn with Asp or Cys in mouse Crys, thus mimicking plant or insect specific Crys, disturbs the function as a clock protein (*35*). Therefore, the

Table 1: Comparison of Amino Acid Residues around FAD

representative	gene cluster	position 386[a]	position 387	position 388	position 392	PDB entry
*S*Cry-DASH	DASH-type Cry	Asp	Tyr	Asp	Asn	1NP7
human Cry1	(6−4) Phr/clock Cry	Asp	Ala	Asp	Asn	not available
Arabidopsis (6−4) Phr	(6−4) Phr/clock Cry	Asp	Ser	Asp	Asn	3FY4
Drosophila Cry	insect specific Cry	Asp[b]	Ala	Asp	Cys	not available
Arabidopsis Cry1	plant specific Cry	Asp	Ala	Asp	Asp	1U3C
E. coli CPD Phr	CPD phr	Asp	Gly	Asp	Asn	1DNP

[a]Numbering in *S*Cry-DASH. [b]Asn in the Cry baby mutant identified in *Drosophila* Cry.

identity of this residue may contribute to cluster, class, or species specific functional roles for Cry/Phr proteins.

Light-induced difference Fourier transform infrared (FTIR) spectroscopy is a useful and powerful method for characterizing structure−function relationships in photoreceptive proteins, as shown for rhodopsins (*36*−*38*). However, only a limited number of FTIR studies are reported for full-length photoreceptors containing flavin cofactors. FTIR was applied to *E. coli* DNA Phr and *Arabidopsis* Cry1, but the Cry/Phr family proteins have been not well assigned (*39*, *40*), as compared to isolated LOV (*25*, *26*, *41*−*47*) and BLUF domains (*32*, *48*−*50*) found in other flavoproteins with distinct folds and unique photoreactions. For application to the spectroscopic system, a solid paradigm with detailed coordinates is essential. In this report, we characterized the photoreaction of Cry-DASH derived from *Synechocystis* sp. PCC6803 (*S*Cry-DASH) by UV−vis and FTIR spectroscopy. In addition to the wild-type protein, we also examined the N392C mutant of *S*Cry-DASH, which mimics insect specific Crys (Table 1 and Figure 1a,d) (*13*, *19*, *20*) in our studies of the photoreaction.

Solution samples are generally not suitable for FTIR analysis; however, we were able to construct an FTIR system using a concentrated solution to measure light-induced difference spectra and applied it to *S*Cry-DASH. Using this system, we identified a signal unique to an anionic form ($FAD^{\bullet-}$) of the protein during the photoreduction process. Substitution of cysteine at the position enriches the $FAD^{\bullet-}$ form. By comparison of difference spectra of $FAD^{\bullet-}$ and FAD^{ox} ($FAD^{\bullet-}/FAD^{ox}$) with those of $FADH^-$ and FAD^{ox} ($FADH^-/FAD^{ox}$), FTIR bands specific to $FAD^{\bullet-}$ and $FADH^-$, respectively, were assigned. We furthermore examined structural changes in the carbonyl group of Asn392 during the $FAD^{\bullet-}$ formation process. In contrast to observations of *Arabidopsis* Cry1 (*40*), no significant signal corresponding to the protonated carboxylic acid moiety was observed for *S*Cry-DASH, suggesting that this contribution is negligible or minor. Thus, we also concluded that while Cry/Phr family proteins also conserve two Asp residues at the FAD binding site (Figure 1a−d and Table 1), an amino acid difference at the Asn position of *S*Cry-DASH is important for the functional diversity observed in plant or insect specific Crys. We discuss potential roles of the position in the Cry/Phr frame.

MATERIALS AND METHODS

Sample Preparation. *Synechocystis* sp. Cry-DASH (*S*Cry-DASH) was expressed in *E. coli* as a fusion protein with glutathione *S*-transferase (GST) at the N-terminus (*6*). After purification of *S*Cry-DASH by glutathione agarose resin (GE Healthcare), the GST tag was cleaved with thrombin. *S*Cry-DASH ($OD_{450} \sim 1.5$) was dissolved in 50 mM Tris-HCl (pH 8), 300 mM NaCl, and 5% (w/v) glycerol and stored at −80 °C until it was used. The N392C mutant of *S*Cry-DASH was constructed by PCR using the QuickChange site-directed mutagenesis method (Stratagene). Nucleotide substitutions were confirmed by DNA sequencing.

UV−Vis Spectroscopy in a Dilute Solution. UV−vis spectra of the diluted *S*Cry-DASH solution were recorded with a V-550DS spectrophotometer (JASCO) at 277 K. *S*Cry-DASH ($OD_{450} \sim 0.15$) in 50 mM Tris-HCl (pH 8), 300 mM NaCl, and 100 mM dithiothreitol (DTT) was transferred into an optical cuvette (path length of 1 cm), deoxygenated by blowing N_2 gas, and sealed with parafilm (Pechiney Plastic Packaging). To initiate the photoreaction, the sample was illuminated with white light using a 1 kW halogen−tungsten lump, and an ND10 filter was used to prevent rapid photoreaction.

UV−Vis and FTIR Spectroscopy in a Concentrated Solution. *S*Cry-DASH ($OD_{450} \sim 1.5$) was concentrated ∼20-fold using a Microcon YM-30 unit (Millipore). After 1.8 μL of concentrated *S*Cry-DASH and 0.2 μL of 1 M DTT were mixed, the solution was put on a BaF_2 window (diameter of 18 mm), sandwiched with another BaF_2 window directly, and sealed with parafilm. H/D exchange was conducted by diluting the *S*Cry-DASH sample with the buffer prepared in D_2O and concentrating three times with an Amicon YM-30 apparatus.

The concentrated solution in BaF_2 windows was measured using UV-550DS and FTS-7000 (Bio-Rad) spectrophotometers equipped with a cryostat (Optistat DN, Oxford, U.K.) and a temperature controller, respectively. The temperature was set at 277 K, and white light illumination with a 1 kW halogen−tungsten lamp was used. For FTIR spectra, 128 interferograms at 2 cm^{-1} resolution were recorded before and after illumination, and seven and five recordings for the wild type and N392C mutant, respectively, were averaged.

RESULTS

In Vitro Photoreduction of SCry-DASH. The FAD cofactor buried within the Cry/Phr protein fold (Figure 1) is subject to redox changes. In the presence of reducing agents, such as 2-mercaptoethanol or DTT in vitro, for example, the cofactor can be reduced in a light-dependent manner (*14*−*17*). To characterize the light-dependent redox changes of FAD in the *S*Cry-DASH protein, we first recorded the light-induced UV−vis spectra of a dilute protein solution (Figure 2a). Under anaerobic conditions in the presence of DTT, white light illumination efficiently converted the redox state from FAD^{ox} to $FADH^-$, after only 4 min (Figure 2a, black solid line). After prolonged illumination for a total of 9 min, we observed an increase in the level of accumulation of the reduced form at 369 nm (Figure 2a, red line). Comparison of the two spectra allows us to estimate the level of accumulation of the reduced form, $FADH^-$. The dotted

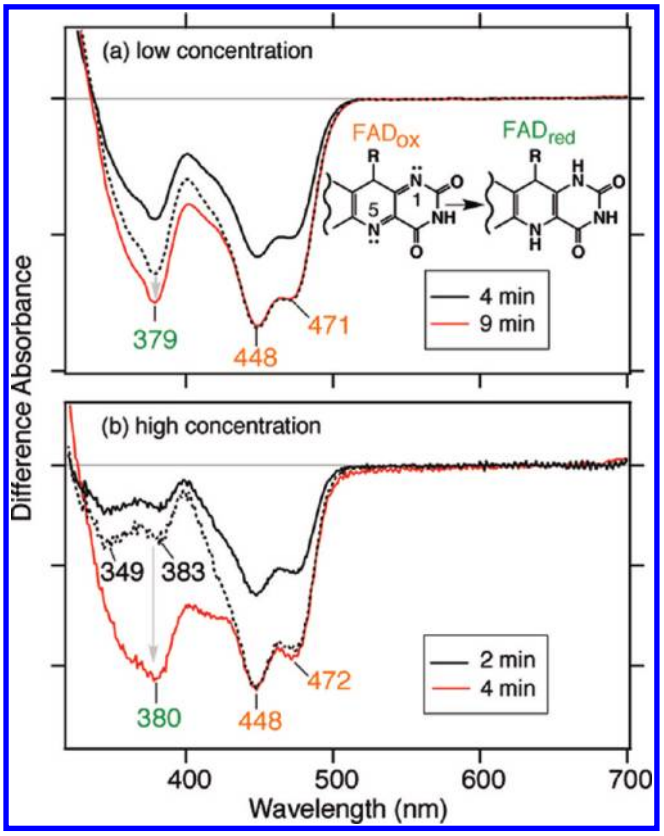

FIGURE 2: Light-induced UV−vis difference spectra upon photoreduction of *S*Cry-DASH. White light illumination was used at (a) low and (b) high protein concentrations in the presence of 100 mM DTT. The low-concentration sample was exposed for 4 or 9 min, while the higher-concentration sample was exposed for 2 or 4 min. In the respective panels, data for the shorter exposure are colored black and data for the longer exposure are colored red. The black dotted line indicates the magnified spectrum of the shorter exposure spectrum (black solid line), 1.45 times for the shorter exposure sample and 1.7 times for the longer exposure sample (see details in the text). One division of the *y*-axis corresponds to 0.04 (a) or 0.005 (b) absorbance unit.

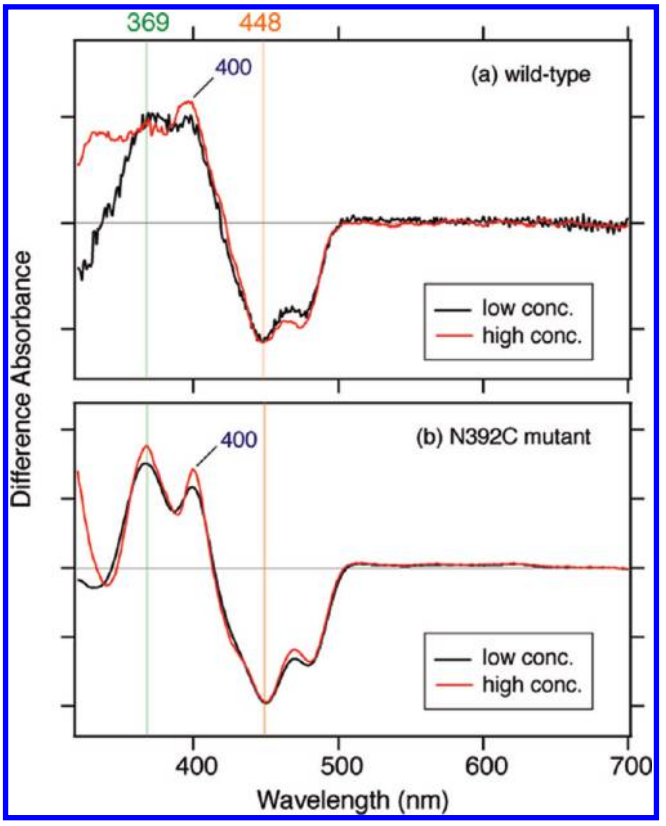

FIGURE 3: Extraction of the $FAD^{\bullet-}$ form in *S*Cry-DASH. (a) Subtraction of adjusted short illumination spectra, containing predominantly the oxidized form, from the long exposure spectra, enriched in the reduced form, revealed a peak characteristic for the anionic form at 400 nm. Data for the dilute condition are colored red, and data for the concentrated sample are colorted black. (b) The *S*Cry-DASH N392C mutant stabilizes the anionic form. Illumination with white light was used out in the presence of 100 mM DTT for 2 min for the low-concentration sample (red line) and 4 min for the high-concentration sample (black line).

line in Figure 2a shows the spectrum, magnified 1.45 times, of the sample exposed for a shorter period of time with negative peaks at 448 and 471 nm, indicative of FAD^{ox}, overlaid onto the prolonged illumination spectrum. The peak intensity at 369 nm of the long exposure sample is significantly larger than that of the magnified spectrum, indicating an accumulation of the reduced form by the longer exposure. The difference in overall intensities may be due to a mixed sample population containing various redox stages of protein. Similar photoreaction could also be observed at the higher concentration used for the FTIR studies as well (Figure 2b). In the difference spectrum of the 2 min illumination, negative peaks at 349 and 383 nm were observed (black lines in Figure 2b).

Ideally, after a short period, various redox states of FAD should exist, while prolonged light exposure will result in homogeneous accumulation of the $FADH^-$ form under anaerobic conditions. However, we did not clearly observe characteristic absorbance at 500−700 nm corresponding to the radical form $FADH^{\bullet}$ or the anionic form $FAD^{\bullet-}$ in the transition from the oxidized to reduced $FADH^-$ (Figure 2). In insect specific Crys, the anionic form, having characteristic absorbance at 400 nm and a smaller peak at 500 nm, was detected in the photoreduction process (*19*, *20*). These intermediate forms may not be stabilized under the conditions or may be masked by the dominant species.

To extract the spectral component, we thus adjusted intensities with the following calculations:

$$\text{corrected intensity} = (\text{intensity ratio of the oxidized form at 448 nm}) \times \text{short exposure} - (\text{intensity ratio of the reduced form at 369 nm}) \times \text{long exposure}$$

where the intensity ratio represents that ratio of the larger intensity to the smaller intensity at 448 nm for the oxidized form and 369 nm for the reduced form.

As shown in Figure 3a, the obtained spectra were distinct from those of the oxidized or reduced form, showing a characteristic peak for the anionic form at 400 nm, though the peak intensity around 500 nm is smaller than those reported (*19*, *20*). Under these conditions, on the basis of the obtained spectrum, we concluded that the short illumination gave 7% $FAD^{\bullet-}$ over $FADH^-$ in a dilute solution, and 62% $FAD^{\bullet-}$ and 38% $FADH^-$ in a concentrated solution (discussed further below). We could not extract $FADH^{\bullet}$ spectra by changing parameters (not shown).

Analysis of Cysteine Mutant SCry-DASH Mimicking Insect Specific Crys. During the redox process in insect specific Crys, the anionic form of FAD is stabilized (*19*, *20*). Notably, the N1 and N5 atoms of the FAD isoalloxazine ring are key for the redox chemistry. Interestingly, insect specific Crys have Cys residues in the vicinity of the N5 atom, such as in plant blue

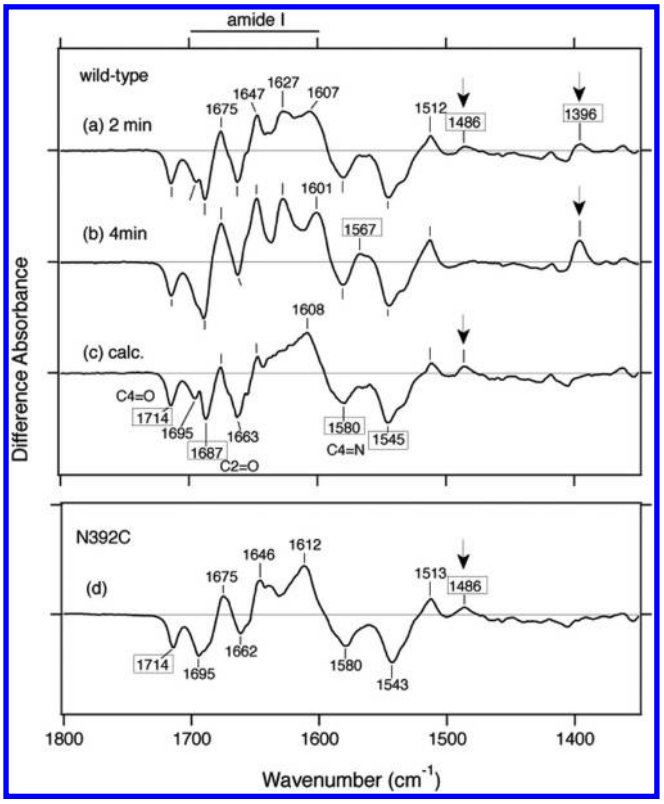

FIGURE 4: Light-induced FTIR difference spectra of wild-type *S*Cry-DASH and the N392C mutant. Light-induced FTIR difference spectra (1800−1350 cm^{-1} region) illustrate additional details of photoreduction. Illumination was conducted at a concentration similar to that for the UV−vis studies for 2 (a) and 4 min (b) in the presence of 100 mM DTT. The calculated spectrum of $FAD^{\bullet-}/FAD^{ox}$ (c) was obtained by subtraction of the magnified short exposure spectrum from the long exposure spectrum, while the exposed spectrum is considered sufficient to represent the difference spectrum of $FADH^{-}/FAD^{ox}$ (see the text for more details). On the basis of the peak intensity at 1714 (−) cm^{-1}, the short exposure spectrum was magnified by 1.3 times to normalize the height to that of the long exposure spectrum for calculation of the difference spectrum of $FADH^{-}/FAD^{ox}$. Lane d shows the difference spectrum of the N392C mutant. One division of the *y*-axis corresponds to 0.006 absorbance unit.

light photoreceptor phototropins, while the N1 atom is exposed (Figure 1d). It is thereby suggested that the presence of cysteine could stabilize the anionic form $FAD^{\bullet-}$ (*19*, *20*). DASH-type Cry proteins, as well as Phrs and mammalian Crys, have Asn at that position (Figure 1a,b and Table 1). Therefore, to investigate the effect of this residue near the isoalloxazine N5 atom on the photoreaction, we measured the photoreaction of the N392C mutant, which mimics insect specific Crys (Figure 1a, d). Figure 3b shows the light-induced UV−vis difference spectra of N392C *S*Cry-DASH in diluted (red line) and concentrated (black line) solutions using short illuminations. Remarkably, we obtained spectra with $FAD^{\bullet-}$ peak intensity well distinguished from that of FAD^{ox} but matching that of insect specific Cry naturally containing Cys as the residue in question (*19*) (Figure 3b). Thus, we concluded that placement of cysteine at position 392 of *S*Cry-DASH can stabilize the anionic form $FAD^{\bullet-}$. Because prolonged illumination resulted in sample precipitation (not shown), we could not confirm whether the N392C mutant is capable of forming $FADH^{-}$. Similar spectra for the wild type and N392C, however, suggest that both *S*Cry-DASH proteins can undergo photoreduction (Figure 3).

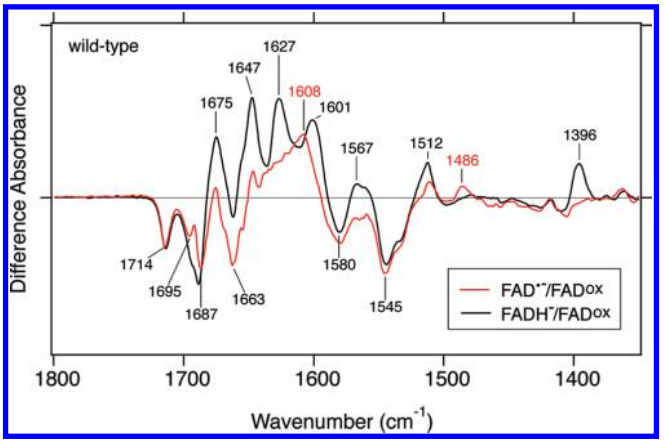

FIGURE 5: Comparison of two difference FTIR spectra of wild-type *S*Cry-DASH. To identify significant peaks, the two different spectra representing $FAD^{\bullet-}/FAD^{ox}$ (red line) and $FADH^{-}/FAD^{ox}$ (black line), taken from panels c and b of Figure 4, respectively, were overlaid in the 1800−1350 cm^{-1} region.

These data imply that the position neighboring the N5 atom of isoalloxazine is critical for the diversity of Cry/Phr family members (Figure 1a−d).

FTIR Spectroscopic Analyses of SCry-DASH. We confirmed that *S*Cry-DASH is capable of responding to light at even relatively high concentrations using UV−vis (Figures 2 and 3). We next analyzed the photoreduction of *S*Cry-DASH in a concentrated solution sandwiched between BaF_2 windows using FTIR spectroscopy. Panels a and b of Figure 4 show the difference FTIR spectra upon 2 and 4 min illumination, respectively, in the 1800−1350 cm^{-1} region. Significant peaks for *S*Cry-DASH were detected at 1714 (−), 1695 (−), 1687 (−), 1675 (+), 1663 (−), 1647 (+), 1627 (+), 1607 (+), 1580 (−), 1545 (−), 1512 (+), 1486 (+), and 1396 (+) cm^{-1}. Overall, the spectra look similar regardless of the exposure time. However, some noticeable differences were found upon longer illumination. When the spectra were normalized to the negative peak at 1714 cm^{-1}, corresponding to the C4═O stretch of FAD (*51*−*55*), peaks in the 1700−1600 cm^{-1} region were sharper in the long exposure spectra than in the short exposure spectra. The positive band at 1486 cm^{-1} disappeared, whereas the positive band at 1396 cm^{-1} increased in intensity with a longer exposure. On the basis of the analyses of the UV−vis difference spectra (Figures 2 and 3), the $FADH^{-}$ state would be predominant with longer illumination, while the short exposure spectrum contains more information about the $FAD^{\bullet-}$ state. Ideally, the results of the FTIR experiments reveal $FAD^{\bullet-}$ and $FADH^{-}$ at a 62:38 ratio, as seen in UV−vis analyses (Figures 2b and 3a). Therefore, to determine the $FAD^{\bullet-}$:FAD^{ox} and $FADH^{-}$:FAD^{ox} ratios from the difference FTIR spectra, we used reference bands, as described below.

The N392C mutant, which exhibits a stable anionic form, can be useful in comparing the $FAD^{\bullet-}$ and FAD^{ox} states of *S*-Cry-DASH. As clearly seen in the UV−vis spectra (Figure 3b), an FTIR spectrum of this mutant could help to distinguish $FAD^{\bullet-}$ from FAD^{ox} under similar conditions. Figure 4d shows the light-induced difference FTIR spectrum of N392C. In the spectrum, there are peaks at 1714 (−), 1695 (−), 1675 (+), 1663 (−), 1646 (+), 1612 (+), 1607 (+), 1580 (−), 1545 (−), 1513 (+), and 1486 (+) cm^{-1}. The FTIR spectrum of the N392C mutant is not entirely coincident with that of the wild type, though some peaks are well-overlapped. Remarkably, the spectra of short exposure

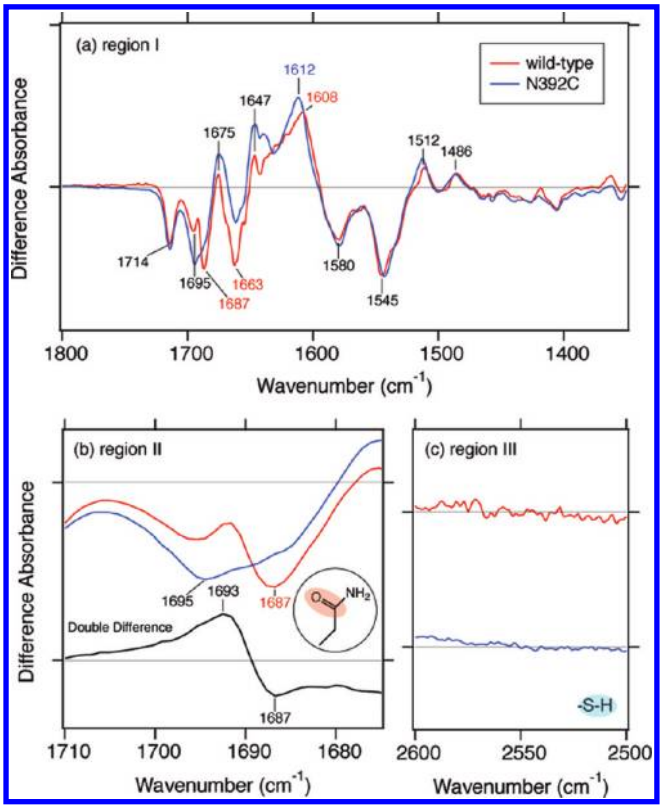

FIGURE 6: Impact of mutations on difference FTIR spectra. Difference FTIR spectra of $FAD^{\bullet-}/FAD^{ox}$ of wild-type *S*Cry-DASH (red line) and the N392C mutant (blue line) were compared in three ranges: (a) 1800−1350, (b) 1720−1670, and (c) 2600−2500 cm^{-1}. Respective data for the wild type and the N392C mutant are identical to data shown in panels c and d of Figure 4, respectively. The bottom black trace in panel b shows the double-difference spectrum between the wild type and the N392C mutant, where the N392C mutant spectrum (blue line) is subtracted from the wild-type spectrum (red line).

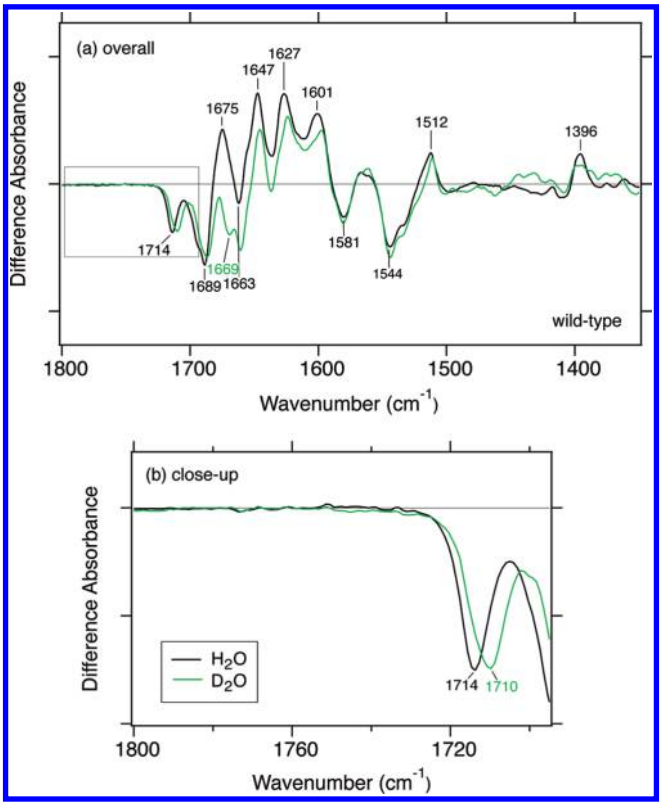

FIGURE 7: Effects of deuterium on photoreduction of *S*Cry-DASH. Difference FTIR spectra of $FADH^{-}/FAD^{ox}$ of wild-type *S*Cry-DASH in H_2O (black line) and D_2O (green line) buffer were compared in the 1800−1350 (a) and 1800−1710 cm^{-1} (b) regions.

wild-type and mutant proteins both exhibit a positive band at 1486 cm^{-1}, which was not observed in the long illumination, whereas the mutant showed no positive band at 1396 cm^{-1} (Figure 4). These results imply that the positive band at 1486 cm^{-1} originates from $FAD^{\bullet-}$, while the positive band at 1396 cm^{-1} is characteristic of the $FADH^{-}$ form.

We then calculated the $FAD^{\bullet-}/FAD^{ox}$ difference FTIR spectrum of wild-type *S*Cry-DASH to control for the peak at 1396 (+) cm^{-1} belonging to $FADH^{-}$ (Figure 4c). Calculation was conducted as follows:

$$\text{adjusted spectrum} = (\text{short illumination spectrum} - 0.4 \times \text{long illumination spectrum})/0.6$$

Consequently, the spectrum of the wild-type protein contains 60% $FAD^{\bullet-}/FAD^{ox}$ and 40% $FADH^{-}/FAD^{ox}$ upon short illumination. This estimation matches well the numbers obtained from UV−vis spectra (Figures 2b and 3a).

Detection of Conformational Changes of SCry-DASH in the Vicinity of FAD. Figure 5 compares the two difference FTIR spectra of $FAD^{\bullet-}/FAD^{ox}$ (red line) and $FADH^{-}/FAD^{ox}$ (black line) of wild-type *S*Cry-DASH. Negative peaks at 1714, 1687, 1580, and 1545 cm^{-1} were common between the two spectra, which presumably originate from vibrations of the FAD^{ox} form. The peaks are assigned as follows: C4=O stretch at 1714 cm^{-1}, C2=O stretch at 1687 cm^{-1}, and C=N stretches at 1580 and 1545 cm^{-1} (*51*−*55*). As described above, positive bands at 1567 and 1396 cm^{-1} are specific to $FADH^{-}$, while a positive band at 1486 cm^{-1} is specific to $FAD^{\bullet-}$. The origins of these positive bands have not yet been identified.

Notably, very different spectral features were observed in the 1700−1600 cm^{-1} region (amide I region), where characteristic frequencies of the C=O stretches of peptide backbone are commonly observed. The $FAD^{\bullet-}/FAD^{ox}$ spectrum shows peaks at 1695 (−), 1687 (−), 1663 (−), 1647 (+), and 1608 (+) cm^{-1}, while the $FADH^{-}/FAD^{ox}$ spectrum has peaks at 1688 (−), 1675 (+), 1647 (+), 1627 (+), and 1601 (+) cm^{-1}. These differences may reflect a secondary structural alteration between the $FAD^{\bullet-}$ and $FADH^{-}$ states, while some of the positive bands may simply indicate C=O stretches of FAD that are independent of the redox status. Interestingly, although the $FAD^{\bullet-}$ and $FADH^{-}$ states are both negatively charged, different FTIR signals strongly suggest that a hydrogen bonding network near the chromophore is significantly affected in inducing conformational changes in the vicinity. The key difference between the two states would be due to the protonation status of the N5 atom of isoalloxazine in FAD (Figure 1).

Regulation of the N5 Atom of the Isoalloxazine Ring of FAD in the Cry/Phr Architecture. To characterize the contribution of the isoalloxazine N5 atom to the conformational change, we compared difference FTIR spectra of the *S*Cry-DASH proteins. Figure 6 compares the $FAD^{\bullet-}/FAD^{ox}$ difference FTIR of the wild-type (red line) and N392C mutant (blue line) *S*Cry-DASH. Overall, spectra of the mutant are similar to those of the wild type, possessing peaks at 1714 (−), 1695 (−), 1675 (+), 1663 (−), 1647 (+), 1580 (−), 1545 (−), 1512 (+), and 1486 (+) cm^{-1}. We observed significant differences in the amide I region (1700−1600 cm^{-1} region), indicating that the substitution

at Asn392 also influenced the light-induced structural changes in the peptide backbone upon the formation of $FAD^{\bullet-}$.

The wild-type spectrum shows negative peaks at 1695 and 1687 cm^{-1}, while the spectrum of the N392C mutant lacks the corresponding negative peak at 1687 cm^{-1} (Figure 6b, top traces). The double-difference spectrum between the wild type and N392C revealed peaks at 1693 (+) and 1687 (−) cm^{-1} (Figure 6b, bottom trace). Generally, C=O stretches of side chains of asparagine and glutamine appear in this region as well as the peptide backbone (amide I vibration). We interpreted that the bands at 1693 (+)/1687 (−) cm^{-1} originate from the C=O stretch of the side chain of Asn392. A shift of the stretching vibrational mode to a higher frequency implies that hydrogen bonding strength of the C=O group is weakened upon formation of $FAD^{\bullet-}$. Figure 6c shows the 2600−2500 cm^{-1} region of the spectra of the wild type and N392C. Normally, the S−H stretch appears in the 2575−2525 cm^{-1} region; however, no such band is observed for the N392C mutant (Figure 6c, blue line). In contrast to those for the wild type, in which Asn392 weakens the hydrogen bond of its C=O side chain, the data indicate that in the hydrogen bonding network of the mutant protein Cys392 does not change upon formation of $FAD^{\bullet-}$. It should be noted that the C4=O stretching frequencies are identical between the N392C mutant and the wild type [1714 cm^{-1} (Figure 6a)]. This suggests that Asn392 does not interact with the N5 atom of FAD in the FAD^{ox} form, because the interaction affects the C4=O band of FAD.

Protonated Carboxylic Acid Residues Are Unnecessary in the Photoreduction of SCry-DASH. For plant specific Cry, carboxylic acid deprotonation was observed in the formation of $FADH^{\bullet}$ (*40*). However, it is unclear which Asp in plant specific Cry contributes to the photoexcitation. Plant specific Crys have Asp. Insect specific Crys have Cys. The rest of the members of the family contain Asn at the position corresponding to Asn392 of *S*Cry-DASH, while the entire family additionally contains two conserved Asp residues (Asp386 and Asp388 in *S*Cry-DASH) near the FAD (Figure 1a−d and Table 1). In *Drosophila*, a mutation of Asp410 to Asn ("cry baby") abolishes the function as a circadian photoreceptor (Figure 1d) (*56*). To investigate the contribution of aspartic acids to the photoreduction, we performed deuterium exchange experiments (Figure 7). Difference FTIR spectra of $FADH^{-}/FAD^{ox}$ of *S*Cry-DASH in H_2O (black line) and D_2O (green line) buffer look similar in the 1800−1350 cm^{-1} region, but with a slight shift in the amide I region, reduced intensity at 1675 (+) cm^{-1}, and a newly appearing band at 1669 (−) cm^{-1} (Figure 7a). In general, C=O stretches of peptide backbone are slightly affected (downshift of 2−3 cm^{-1}) by the H/D exchange in the N−H groups. However, the C2=O stretch of FAD^{ox} shows a downshift of >10 cm^{-1} caused by the deuteration of the N3−H group (*53*−*55*), and the negative band at 1669 cm^{-1} might originate from a C2=O stretch. The band intensity at 1396 (+) cm^{-1} is slightly reduced in the D_2O buffer. H/D exchangeable groups in the FAD are the N3−H (in the FAD^{ox} and $FADH^{-}$ forms) and N5−H (in the $FADH^{-}$ form) groups. The positive band at 1396 cm^{-1} may include a N−H bending vibration of FAD. The negative band at 1714 cm^{-1} probably originates from a C4=O stretch of the FAD^{ox} form (Figure 7b). The 4 cm^{-1} spectral shift in the D_2O buffer may be due to an indirect effect of the deuteration of the N3H group (*53*−*55*). For *S*Cry-DASH, no significant signal was observed in the 1800−1720 cm^{-1} region. This implies that the FAD reduction process of *S*Cry-DASH does not involve structural changes of protonated carboxylic acid residues by protonaton and/or deprotonation, or hydrogen bond alteration. The difference would likely arise from the distinct residues in the vicinity of the N5 atom of FAD (Figure 1a,c).

DISCUSSION

Adaptations to light are diverse in different organisms, and chemical reactions triggered by light are subtle but critical. Unlike other photoreceptors, such as rhodopsin (retinal), phytochrome (bilin), or photoactive yellow protein (coumaric acid), drastic *cis*−*trans* chemical conformational change is not expected in flavin-bound blue light photoreceptors containing planar isoalloxazine rings. Light-dependent conformational assembly changes and dissociations have been proposed for the flavin-based photoreceptors such as Crys and LOV and BLUF domain proteins. Fully understanding how light is captured, resulting in such structural rearrangement for signaling, however, requires detailed characterizations of the chromophore and its vicinity in both the ground and excited states. Three-dimensional structural information about Cry/Phr family proteins has revealed a similar overall fold and conserved mode of chromophore binding, and light activation of FAD has been discussed; however, signal conversion (i.e., FAD-driven protein dynamics) remains unclear. For this reason, it is essential to couple information about the FAD redox state to contributions of identified interaction sites. In a light- and time-dependent process (Figure 2), we extracted a signal for the anionic form $FAD^{\bullet-}$ as one of the intermediates (Figure 3a).

Several recent studies of FAD redox states in Cry-DASHs have been reported (*14*−*16*). Damiani et al. showed that *S*Cry-DASH can form $FADH^{\bullet}$ (*16*). Biskup et al. and Damiani et al. also both showed that $FADH^{\bullet}$ accumulates not via photoreaction but via oxidation of the light-induced reduced form (*14*, *15*). In contrast, here we detected $FAD^{\bullet-}$, not $FADH^{\bullet}$, upon light illumination. We infer that the stable redox states that arise from the processes of photoreduction and oxygen-induced oxidation are distinct. Our data are also in contrast to those of Zikihara et al. (*14*), in which they observed $FADH^{\bullet}$ upon light illumination. Indeed, stable intermediates may be different between Cry-DASHs of *Synechocystis* and zebrafish. The molecular mechanisms of these unique reaction pathways are intriguing and await further characterization.

Mutation of Asn392 to Cys, which mimics *Drosophila* Cry, stabilized the $FAD^{\bullet-}$ form (Figure 3b). As represented by the structure of *S*Cry-DASH (Figure 1a), in many Cry and Phr proteins, the neutral Asn (Asn392 of *S*Cry-DASH) interacts with the N5 position of the FAD isoalloxazine, whereas insect and plant specific Crys have Cys and Asp, respectively (Figure 1b−d). Phrs and most Crys are believed to form $FADH^{\bullet}$ and $FADH^{-}$ (*2*, *14*−*17*, *33*, *40*), while insect Crys form stable $FAD^{\bullet-}$ (*19*, *20*). As it is thought that Asn or Asp at the position can control the redox state of FAD (*33*), the Cys is also positioned aptly to be involved in the redox state of FAD.

The Asn is highly conserved in DASH-type Crys, Phrs, and also mammalian clock-related Crys (Table 1). This key conserved Asn is crucial for both (i) DNA repair Phrs in restoring normal bases from UV-induced photoproducts in DNA strands and (ii) mammalian clock-related Crys in repressing transcriptional activation by the BMAL1−CLOCK complex through the E-box contents in DNA as part of a negative feedback loop (Figure 1 and Table 1). Substitution of the Asn in mammalian Crys with Cys or Asp, mimicking insect or plant specific Crys, respectively,

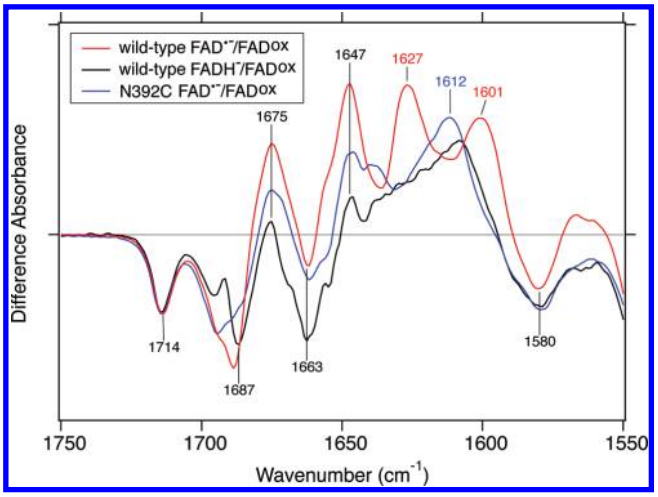

FIGURE 8: Overlaid difference FTIR spectra of wild-type *S*Cry-DASH and the N392C mutant. Three different spectra in Figure 4 (lanes b−d) were overlaid in the 1750−1550 cm^{-1} region. $FAD^{\bullet-}/FAD^{ox}$ and $FADH^{-}/FAD^{ox}$ spectra of wild-type *S*Cry-DASH are shown as red and black lines, respectively, while the $FAD^{\bullet-}/FAD^{ox}$ spectrum of the N392C mutant is shown as a blue line.

disturbs the suppression activity in the clock system, indicating that the residue is one of the keys for the functional diversity of the Cry/Phr family. Genetic approaches have revealed that *Drosophila* Cry and mammalian Crys are both involved in the maintenance of robust daily rhythms, but their essential roles in the circadian rhythms are quite different. The insect specific Cry has been considered as a primary photoreceptor. This was supported by an identified mutant named cry baby, which has a substitution at one of the Asp residues conserved among members of the Cry/Phr family (Figure 1d) (*56*).

Our FTIR spectral data illustrate that *S*Cry-DASH can exist in several distinct FAD states, including FAD^{ox} and $FADH^{-}$ (Figures 4−6). The detection of the anion form indicates that the transfer of a proton to the chromophore, but not primary electron transfer, would likely take place in *S*Cry-DASH. Successfully, we obtained $FAD^{\bullet-}/FAD^{ox}$ and $FADH^{-}/FAD^{ox}$ FTIR difference spectra of *S*Cry-DASH in the 1800−1350 and 2600−2500 cm^{-1} regions, allowing assignment of characteristic peaks. The C═O stretch of the Asn392 side chain weakened the hydrogen bonding in the $FAD^{\bullet-}$ state of the wild type (Figure 6a, b). Because the C═O side chain of Asn392 forms a hydrogen bond with Trp396 (Figure 1), the simplest interpretation is that the distance between Asn392 and Trp396 is further in the $FAD^{\bullet-}$ state. Near the chromophore, the Cry/Phr family proteins contain a highly conserved Trp triad chain (Trp396-Trp373-Trp320 of *S*Cry-DASH), originally identified in *E. coli* DNA Phr (Figure 1e) (*15*), that is thought to be an electron transfer pathway. Trp396 of the *S*Cry-DASH triad is closest to the FAD. The negative charge of $FAD^{\bullet-}$ could affect the surrounding environment. On the other hand, the S−H group of Cys392 in the N392C mutant did not change its hydrogen bonding environment (Figure 6c). In the N392C mutant, the S−H group may face Ala377 and Trp393 (see Figure 1). Asn392 plays an important role in the transfer of electrons and protons into $FAD^{\bullet-}$ for the second electron transfer process, conversion from $FAD^{\bullet-}$ to $FADH^{-}$. The hydrogen bonding environment of Asn392 should be crucial for the step. The substituted Cys residue may not directly interact with the FAD chromophore. This does not necessarily mean that there would be no interaction between the cysteine and FAD in insect specific Crys (Figure 1d) as seen in the N392C mutant of *S*Cry-DASH, while the anion form is stabilized rather than the radical form in the insect Crys (*19*). Figure 8 compares the $FAD^{\bullet-}/FAD^{ox}$ spectrum of the N392C mutant (blue line) with the $FAD^{\bullet-}/FAD^{ox}$ (black line) and $FADH^{-}/FAD^{ox}$ (red line) spectra of wild-type *S*Cry-DASH. The $FAD^{\bullet-}/FAD^{ox}$ spectrum of N392C is located between the $FAD^{\bullet-}/FAD^{ox}$ and $FADH^{-}/FAD^{ox}$ spectra of the wild type in the 1680−1640 cm^{-1} region, while quite different features appear in the 1640−1600 cm^{-1} region, especially between $FAD^{\bullet-}/FAD^{ox}$ of N392C and $FADH^{-}/FAD^{ox}$ of the wild type. It would be reasonable that the spectral shapes would be different between them if the C═O stretches of $FAD^{\bullet-}$ or $FADH^{-}$ appear in the 1640−1600 cm^{-1} region. Nevertheless, judging from the spectra in the 1640−1600 cm^{-1} region, the N392C mutant structure in the $FAD^{\bullet-}$ state may have hybrid features between those of the $FAD^{\bullet-}$ and $FADH^{-}$ states of wild-type *S*Cry-DASH, though the difference must originate from the interaction of the amino acid residue at position 392.

We assume that the N392C mutant cannot proceed further to the $FADH^{-}$ state, because the N392C structure in the $FAD^{\bullet-}$ state may be closer to that of the $FADH^{-}$ state of the wild type. Unlike that of the wild type, the S−H group of the substituted Cys would not interact with the neighbor Trp residue in the N392C mutant. Therefore, the mutant would not change its hydrogen bonding environment much upon formation of the $FAD^{\bullet-}$ state (Figure 6c). Notably, this structure may partially mimic that of the $FADH^{-}$ state of the wild type. If this is the case, the hydrogen bonding interaction between Asn392 and Trp396 may be weaker in the $FADH^{-}$ state than in the $FAD^{\bullet-}$ state. That is, protonation of the N5 atom of FAD in the $FADH^{-}$ state would strengthen the interaction between the polypeptide and FAD by forming a hydrogen bond between Asn392 and the N5 position of isoalloxazine.

Our studies of *S*Cry-DASH indicate that FAD is not protonated from a nearby carboxylic acid residue upon formation of $FADH^{-}$ (Figure 7b). This may seem to be in contrast to the FTIR study of *Arabidopsis* Cry1, in which the aspartic acid residue donates a proton for the formation of $FADH^{\bullet}$ (*40*). Kottke et al. suggested that the origin of the proton is Asp396 whose position corresponds to Asn392 in *S*Cry-DASH, but other possibilities cannot be excluded, as the Cry/Phr family proteins (including DASH-type and plant specific Crys) contain two highly conserved Asp residues at the FAD binding site (Figure 1a,c; Asp386 and Asp388 in *S*Cry-DASH and Asp390 and Asp392 in *Arabidopsis* Cry1). However, our results best support such a role for Asp396 of *Arabidopsis* Cry1, corresponding to Asn392 of *S*Cry-DASH, whereas the other two Asp residues would function uniquely for the light response.

CONCLUSION

We examined different FAD redox states of *S*Cry-DASH by UV−vis and FTIR spectroscopy. The results not only identified a key role for the Asn highly conserved among Cry/Phr proteins, including mammalian clock-related Crys, but also ruled out two conserved Asp residues at the FAD binding site as hydrogen donors, demonstrating functional diversity and a critical role at the site in plant and insect specific Crys.

ACKNOWLEDGMENT

We thank Dr. Haruki Nakamura for modeling advice for *Drosophila* cryptochrome, Chiharu Hitomi for technical assistance, and Ashley Pratt for critical reading of the manuscript.

REFERENCES

1. Lin, C., and Todo, T. (2005) The cryptochromes. *Genome Biol. 6*, No. Article 220.
2. Sancar, A. (2003) Structure and function of DNA photolyase and cryptochrome blue-light photoreceptors. *Chem. Rev. 103*, 2203–2237.
3. Cashmore, A. R. (2003) Cryptochromes: Enabling plants and animals to determine circadian time. *Cell 114*, 537–543.
4. Ahmad, M., Grancher, N., Heil, M., Black, R. C., Giovani, B., Galland, P., and Lardemer, D. (2002) Action spectrum for cryptochrome-dependent hypocotyl growth inhibition in *Arabidopsis*. *Plant Physiol. 129*, 774–785.
5. Bouly, J.-P., Schleicher, E., Dionisio-Sese, M., Vandenbussche, F., Van Der Straeten, D., Bakrim, N., Meier, S., Batschauer, A., Galland, P., Bittl, R., and Ahmad, M. (2007) Cryptochrome blue light photoreceptors are activated through interconversion of flavin redox states. *J. Biol. Chem. 282*, 9383–9391.
6. Hitomi, K., Okamoto, K., Daiyasu, H., Miyashita, H., Iwai, S., Toh, H., Ishiura, M., and Todo, T. (2000) Bacterial cryptochrome and photolyase: Characterization of two photolyase-like genes of *Synechocystis* sp. PCC6803. *Nucleic Acids Res. 28*, 2353–2362.
7. Daiyasu, H., Ishikawa, T., Kuma, K., Iwai, S., Todo, T., and Toh, H. (2004) Identification of cryptochrome DASH from vertebrates. *Genes Cells 9*, 479–495.
8. Froehlich, A. C., Chen, C.-H., Belden, W. J., Madeti, C., Roenneberg, T., Merrow, M., Loros, J. J., and Dunlap, J. C. (2010) Genetic and molecular characterization of a cryptochrome from the filamentous fungus *Neurospora crassa*. *Eukaryotic Cell 9*, 738–750.
9. Selby, C. P., and Sancar, A. (2006) A cryptochrome/photolyase class of enzymes with single-stranded DNA-specific photolyase activity. *Proc. Natl. Acad. Sci. U.S.A. 103*, 17696–17700.
10. Pokorny, R., Klar, T., Hennecke, U., Carell, T., Batschauer, A., and Essen, L.-O. (2008) Recognition and repair of UV lesions in loop structures of duplex DNA by DASH-type cryptochrome. *Proc. Natl. Acad. Sci. U.S.A. 105*, 21023–21027.
11. Coesel1, S., Mangogna, M., Ishikawa, T., Heijde, M., Rogato, A., Finazzi, G., Todo, T., Bowler, C., and Falciatore, A. (2009) Diatom PtCPF1 is a new cryptochrome/photolyase family member with DNA repair and transcription regulation activity. *EMBO Rep. 10*, 655–661.
12. Brudler, R., Hitomi, K., Daiyasu, H., Toh, H., Kucho, K., Ishiura, M., Kanehisa, M., Roberts, V. A., Todo, T., Tainer, J. A., and Getzoff, E. D. (2003) Identification of a new cryptochrome class: Structure, function, and evolution. *Mol. Cell 11*, 59–67.
13. Huang, Y., Baxter, R., Smith, B. S., Partch, C. L., Colbert, C. L., and Deisenhofer, J. (2006) Crystal structure of cryptochrome 3 from *Arabidopsis thaliana* and its implication for photolyase activity. *Proc. Natl. Acad. Sci. U.S.A. 103*, 17701–17706.
14. Zikihara, K., Ishikawa, T., Todo, T., and Tokutomi, S. (2008) Involvement of electron transfer in the photoreaction of zebrafish cryptochrome-DASH. *Photochem. Photobiol. 84*, 1016–1023.
15. Biskup, T., Schleicher, E., Okafuji, A., Link, G., Hitomi, K., Getzoff, E. D., and Weber, S. (2009) Direct observation of a photoinduced radical pair in a cryptochrome blue-light photoreceptor. *Angew. Chem., Int. Ed. 48*, 404–407.
16. Damiani, M. J., Yalloway, G. N., Lu, J., McLeod, N. R., and O'Neill, M. A. (2009) Kinetic stability of the flavin semiquinone in photolyase and cryptochrome-DASH. *Biochemistry 48*, 11399–11411.
17. Weber, S., Biskup, T., Okafuji, A., Marino, A. R., Berthold, T., Link, G., Hitomi, K., Getzoff, E. D., Schleicher, E., and Norris, J. R. (2010) Origin of light-induced spin-correlated radical pairs in cryptochrome. *J. Phys. Chem. B* DOI: 10.1021/jp103401u.
18. Payne, G., Heelis, P. F., Rohrs, B. R., and Sancar, A. (1987) The active form of *Escherichia coli* DNA photolyase contains a fully reduced flavin and not a flavin radical, both in vivo and in vitro. *Biochemistry 26*, 7121–7127.
19. Berndt, A., Kottke, T., Breitkreuz, H., Dvorsky, R., Hennig, S., Alexander, M., and Wolf, E. (2007) A novel photoreaction mechanism for the circadian blue light photoreceptor *Drosophila* cryptochrome. *J. Biol. Chem. 282*, 13011–13021.
20. Öztürk, N., Song, S.-H., Selby, C. P., and Sancer, A. (2008) Animal type 1 cryptochromes. *J. Biol. Chem. 283*, 3256–3263.
21. Salomon, M., Christie, J. M., Knieb, E., Lempert, U., and Briggs, W. R. (2000) Photochemical and mutational analysis of the FMN-binding domains of the plant blue light receptor, phototropin. *Biochemistry 39*, 9401–9410.
22. Swartz, T. E., Corchnoy, S. B., Christie, J. M., Lewis, J. W., Szundi, I., Briggs, W. R., and Bogomolni, R. A. (2001) The photocycle of a flavin-binding domain of the blue light photoreceptor phototropin. *J. Biol. Chem. 276*, 36493–36500.
23. Salomon, M., Eisenreich, W., Durr, H., Schleicher, E., Knieb, E., Massey, V., Rudiger, W., Muller, F., Bacher, A., and Richter, G. (2001) An optomechanical transducer in the blue light receptor phototropin from *Avena sativa*. *Proc. Natl. Acad. Sci. U.S.A. 98*, 12357–12361.
24. Crosson, S., and Moffat, K. (2002) Photoexcited structure of a plant photoreceptor domain reveals a light-driven molecular switch. *Plant Cell 14*, 1067–1075.
25. Nozaki, D., Iwata, T., Ishikawa, T., Todo, T., Tokutomi, S., and Kandori, H. (2004) Role of Gln1029 in the photoactivation processes of the LOV2 domain in *Adiantum* phytochrome3. *Biochemistry 43*, 8373–8379.
26. Iwata, T., Nozaki, D., Tokutomi, S., Kagawa, T., Wada, M., and Kandori, H. (2003) Light-induced structural changes in the LOV2 domain of *Adiantum* phytochrome3 studied by low-temperature FTIR and UV-visible spectroscopy. *Biochemistry 42*, 8183–8191.
27. Harper, S. M., Christie, J. M., and Gardner, K. H. (2004) Disruption of the LOV-Jα helix interaction activates phototropin kinase activity. *Biochemistry 43*, 16184–16192.
28. Jones, M. A., Feeney, K. A., Kelly, S. M., and Christie, J. M. (2007) Mutational analysis of phototropin 1 provides insights into the mechanism underlying LOV2 signal transmission. *J. Biol. Chem. 282*, 6405–6414.
29. Yamamoto, A., Iwata, T., Sato, Y., Matsuoka, D., Tokutomi, S., and Kandori, H. (2009) Light signal transduction pathway from flavin chromophore to Jα helix of *Arabidopsis* phototropin1. *Biophys. J. 96*, 2771–2778.
30. Kita, A., Okajima, K., Morimoto, Y., Ikeuchi, M., and Miki, K. (2005) Structure of cyanobacterial BLUF protein, Tll0078, containing a novel FAD-binding blue light sensor domain. *J. Mol. Biol. 349*, 1–5.
31. Ito, S., Murakami, A., Sato, K., Nishina, Y., Shiga, K., Takahashi, T., Higashi, S., Iseki, M., and Watanabe, M. (2005) Photocycle features of heterologously expressed and assembled eukaryotic flavin-binding BLUF domains of photoactivated adenylyl cyclase (PAC), a blue-light receptor in *Euglena gracilis*. *Photochem. Photobiol. Sci. 4*, 762–769.
32. Okajima, K., Fukushima, Y., Suzuki, H., Kita, A., Ochiai, Y., Katayama, M., Shibata, Y., Miki, K., Noguchi, T., Itoh, S., and Ikeuchi, M. (2006) Fate determination of the flavin photoreceptions in the cyanobacterial blue light receptor TePixD (Tll0078). *J. Mol. Biol. 363*, 10–18.
33. Balland, V., Byrdin, M., Eker, A. P. M., Ahmad, M., and Brettel, K. (2009) What makes the difference between a cryptochrome and DNA photolyase? A spectroelectrochemical comparison of the flavin redox transitions. *J. Am. Chem. Soc. 131*, 426–427.
34. Xu, L., Mu, W., Ding, Y., Luo, Z., Han, Q., Bi, F., Wang, Y., and Song, Y. (2008) Active site of *Escherichia coli* DNA photolyase: Asn378 is crucial both for stabilizing the neutral flavin radical cofactor and for DNA repair. *Biochemistry 47*, 8736–8743.
35. Hitomi, K., DiTacchio, L., Arvai, A. S., Yamamoto, J., Kim, S. T., Todo, T., Tainer, J. A., Iwai, S., Panda, S., and Getzoff, E. D. (2009) Functional motifs in the (6−4) photolyase crystal structure make a comparative framework for DNA repair photolyases and clock cryptochromes. *Proc. Natl. Acad. Sci. U.S.A. 106*, 6962–6967.
36. Siebert, F. (1995) Infrared spectroscopy applied to biochemical and biological problems. *Methods Enzymol. 246*, 501–526.
37. Kandori, H. (2000) Role of internal water molecules in bacteriorhodopsin. *Biochim. Biophys. Acta 1460*, 177–191.
38. Kandori, H. (2004) Hydrogen switch model for the proton transfer in the Schiff base region of bacteriorhodopsin. *Biochim. Biophys. Acta 1658*, 72–79.
39. Schleicher, E., Hesssling, B., Illarionova, V., Bacher, A., Weber, S., Richter, G., and Gerwert, K. (2005) Light-induced reactions of *Escherichia coli* DNA photolyase monitored by Fourier transform infrared spectroscopy. *FEBS J. 272*, 1855–1866.
40. Kottke, T., Batschauer, A., Ahmad, M., and Heberle, J. (2006) Blue-light-induced changes in *Arabidopsis* cryptochrome 1 probed by FTIR difference spectroscopy. *Biochemistry 45*, 2472–2479.
41. Swartz, T. E., Wenzel, P. J., Corchnoy, S. B., Briggs, W. R., and Bogomolni, R. A. (2002) Vibration spectroscopy reveals light-induced chromophore and protein structural changes in the LOV2 domain of the plant blue-light receptor phototropin 1. *Biochemistry 41*, 7183–7189.
42. Iwata, T., Tokutomi, S., and Kandori, H. (2002) Photoreaction of the cysteine S−H group in the LOV2 domain of *Adiantum* phytochrome3. *J. Am. Chem. Soc. 124*, 11840–11841.
43. Ataka, K., Hegemann, P., and Heberle, J. (2003) Vibrational spectroscopy of an algal phot-LOV1 domain probes the molecular changes associated with blue-light reception. *Biophys. J. 84*, 466–474.

44. Iwata, T., Nozaki, D., Tokutomi, S., and Kandori, H. (2005) Comparative investigation of the LOV1 and LOV2 domains in *Adiantum* phytochrome3. *Biochemistry 44*, 7427–7434.
45. Iwata, T., Nozaki, D., Sato, Y., Sato, K., Nishina, Y., Shiga, K., Tokutomi, S., and Kandori, H. (2006) Identification of the C═O stretching vibrations of FMN and peptide backbone by ^{13}C-labeling of the LOV2 domain of *Adiantum* phytochrome3. *Biochemistry 45*, 15384–15391.
46. Yamamoto, A., Iwata, T., Tokutomi, S., and Kandori, H. (2008) Role of Phe1010 in light-induced structural changes of the neo1-LOV2 domain of *Adiantum*. *Biochemistry 47*, 922–928.
47. Koyama, T., Iwata, T., Yamamoto, A., Sato, Y., Matsuoka, D., Tokutomi, S., and Kandori, H. (2009) Different Role of the Jα Helix in the Light-Induced Activation of the LOV2 Domains in Various Phototropins. *Biochemistry 48*, 7621–7628.
48. Masuda, S., Hasegawa, K., Ishii, A., and Ono, T. (2004) Light-induced structural changes in a putative blue-light receptor with a novel FAD binding fold sense of blue-light using FAD (BLUF); slr1694 of *Synechocystis* sp. PCC6803. *Biochemistry 43*, 5304–5313.
49. Masuda, S., Hasegawa, K., and Ono, T. (2005) Light-induced structural changes of apoprotein and chromophore in the sensor of blue light using FAD (BLUF) domain of AppA for a signaling state. *Biochemistry 44*, 1215–1224.
50. Hasegawa, K., Masuda, S., and Ono, T. (2006) Light induced structural changes of a full-length protein and its BLUF domain in YcgF (Blrp), a blue-light sensing protein that use FAD (BLUF). *Biochemistry 45*, 3785–3793.
51. Bowman, W. D., and Spiro, T. G. (1981) Normal mode analysis of lumiflavin and interpretation of resonance Raman spectra of flavoproteins. *Biochemistry 20*, 3313–3318.
52. Schmidt, J., Coudron, P., Thompson, A. W., Watters, K. L., and McFarland, J. T. (1983) Assignment and the effect of hydrogen bonding on the vibrational normal modes of flavins and flavoproteins. *Biochemistry 22*, 76–84.
53. Abe, M., and Kyogoku, Y. (1987) Vibrational analysis of flavin derivatives: Normal coordinate treatments of lumiflavin. *Spectrochim. Acta 43A*, 1027–1038.
54. Livery, C. R., and McFarland, J. T. (1990) Assignment and the effect of hydrogen bonding on the vibrational normal modes of flavins and flavoproteins. *J. Phys. Chem. 94*, 3980–3994.
55. Zhang, W., Vivoni, A., Lombard, J. R., and Birke, R. L. (1995) Time-resolved SERS study of direct photochemical charge transfer between FMN and a Ag electrode. *J. Phys. Chem. 99*, 12846–12857.
56. Stanewsky, R., Kaneko, M., Emery, P., Beretta, B., Wager-Smith, K., Kay, S. A., Rosbash, M., and Hall, J. C. (1998) The *cry^b* mutation identifies cryptochrome as a circadian photoreceptor in *Drosophila*. *Cell 95*, 681–692.
57. DeLano, W. L. (2002) The PyMOL molecular graphics system, DeLano Scientific, San Carlos, CA.